New Phytologist

Research

ZmMADS69 functions as a flowering activator through the *ZmRap2.7-ZCN8* regulatory module and contributes to maize flowering time adaptation

Yameng Liang[1]*, Qiang Liu[2]*, Xufeng Wang[1,3]*, Cheng Huang[1,4], Guanghui Xu[1], Stefan Hey[2], Hung-Ying Lin[2], Cong Li[1], Dingyi Xu[1], Lishuan Wu[1], Chenglong Wang[1], Weihao Wu[1], Jinliang Xia[1], Xu Han[1], Sijia Lu[5], Jinsheng Lai[1], Weibin Song[1], Patrick S. Schnable[2,6] and Feng Tian[1]

[1]National Maize Improvement Center of China, Key Laboratory of Biology and Genetic Improvement of Maize (MOA), Beijing Key Laboratory of Crop Genetic Improvement, China Agricultural University, Beijing 100193, China; [2]Department of Agronomy, Iowa State University, Ames, IA 50010-3650, USA; [3]Guangdong Provincial Key Laboratory for Plant Epigenetics, College of Life Sciences and Oceanography, Shenzhen University, Shenzhen, China; [4]College of Agronomy, Hunan Agricultural University, Changsha 410128, China; [5]School of Life Sciences, Guangzhou University, Guangzhou 510006, China; [6]Department of Plant Genetics & Breeding, China Agricultural University, Beijing 100193, China

Authors for correspondence:
Feng Tian
Tel: +86 010 62734660
Email: ft55@cau.edu.cn

Patrick S. Schnable
Tel: +1 515 294 0975
Email: schnable@iastate.edu

Weibin Song
Tel: +86 010 627314641
Email: songwb@cau.edu.cn

Received: *9 August 2018*
Accepted: *14 September 2018*

New Phytologist (2019) **221:** 2335–2347
doi: 10.1111/nph.15512

Key words: adaptation, flowering time, maize, teosinte, *ZCN8*, *ZmMADS69*, *ZmRap2.7*.

Summary

- Flowering time is a major determinant of the local adaptation of plants. Although numerous loci affecting flowering time have been mapped in maize, their underlying molecular mechanisms and roles in adaptation remain largely unknown.
- Here, we report the identification and characterization of MADS-box transcription factor *ZmMADS69* that functions as a flowering activator through the *ZmRap2.7-ZCN8* regulatory module and contributes to adaptation. We show that *ZmMADS69* underlies a quantitative trait locus controlling the difference in flowering time between maize and its wild ancestor, teosinte. Maize *ZmMADS69* allele is expressed at a higher level at floral transition and confers earlier flowering than the teosinte allele under long days and short days. Overexpression of *ZmMADS69* causes early flowering, while a transposon insertion mutant of *ZmMADS69* exhibits delayed flowering. *ZmMADS69* shows pleiotropic effects for multiple traits of agronomic importance.
- *ZmMADS69* functions upstream of the flowering repressor *ZmRap2.7* to downregulate its expression, thereby relieving the repression of the florigen gene *ZCN8* and causing early flowering. Population genetic analyses showed that *ZmMADS69* was a target of selection and may have played an important role as maize spread from the tropics to temperate zones.
- Our findings provide important insights into the regulation and adaptation of flowering time.

Introduction

Maize (*Zea mays* ssp. *mays*) was domesticated in southwestern Mexico *c.* 9000 yr ago from its wild progenitor, teosinte (*Zea mays* ssp. *parviglumis*) (Matsuoka *et al.*, 2002). During domestication, maize underwent a dramatic transformation in plant and inflorescence architecture relative to teosinte (Doebley, 2004). In addition to the dramatic morphological differences, maize and teosinte also differ substantially in geographical distribution and local adaptation. Teosinte was restricted to tropical environments in Mexico and Central America, while maize spread over 90° of latitude and has become one of the world's most widely cultivated crops (Hung *et al.*, 2012; Huang *et al.*, 2018), which was made possible mainly via the adaptation of flowering time to local environments.

Most knowledge on factors controlling flowering time was gained from research in *Arabidopsis* and rice (Shrestha *et al.*, 2014; Blümel *et al.*, 2015). By contrast, the understanding of the genetic controls of flowering time in maize is limited. Several key genes affecting maize flowering have been cloned through mutant analysis and comparative genomics (Dong *et al.*, 2012). *INDETERMINATE1* (*ID1*) encodes a monocot-specific zinc finger transcription factor that functions through the autonomous pathway to promote flowering (Colasanti *et al.*, 1998). *DELAYED FLOWERING1* (*DLF1*) is another key gene that is required for the floral transition in maize and functions downstream of *ID1* (Muszynski *et al.*, 2006). *DLF1* encodes a bZIP

*These authors contributed equally to this work.

protein (Muszynski *et al.*, 2006) that is homologous to *FLOWERING LOCUS D* (*FD*) of *Arabidopsis* (Abe *et al.*, 2005; Wigge *et al.*, 2005). The identification of the most likely maize florigen gene *ZEA CENTRORADIALIS 8* (*ZCN8*) among multiple maize *FT*-like genes is a breakthrough in understanding flowering time regulation in maize (Lazakis *et al.*, 2011; Meng *et al.*, 2011). *ZCN8* is transcribed and translated in the leaf vasculature and then moves through the phloem to the shoot apical meristem (SAM) where it interacts with DLF1 protein to activate downstream floral organ identity genes (Lazakis *et al.*, 2011; Meng *et al.*, 2011). *ZmMADS1* is an ortholog of the central flowering integrator *SUPPRESSOR OF OVEREXPRESSION OF CONSTANS1* (*SOC1*) of *Arabidopsis* and functions as a flowering activator in maize (Alter *et al.*, 2016). *ZEA MAYS MADS4* (*ZMM4*) is a floral meristem identity gene that involves both floral induction and inflorescence development (Danilevskaya *et al.*, 2008).

Maize exhibits tremendous natural diversity in flowering time (Kuleshov, 1933; Buckler *et al.*, 2009). To identify genetic factors controlling the natural variation in flowering time, extensive mapping studies have been conducted using various mapping populations (Austin & Lee, 1996; Ribaut *et al.*, 1996; Salvi *et al.*, 2002; Chardon *et al.*, 2004; Briggs *et al.*, 2007; Buckler *et al.*, 2009; Coles *et al.*, 2010; Hung *et al.*, 2012; Steinhoff *et al.*, 2012; Romay *et al.*, 2013; Yang *et al.*, 2013; X. Y. Li *et al.*, 2016; Romero Navarro *et al.*, 2017; Jin *et al.*, 2018). The results showed that flowering time in maize is controlled by a complex genetic architecture, with numerous small-effect quantitative trait loci (QTLs) involved (Buckler *et al.*, 2009; X. Y. Li *et al.*, 2016). Due to this complexity, to date, only a few flowering time QTLs have been cloned. *Vegetative to generative transition 1* (*Vgt1*) is the first cloned flowering time QTL in maize, which has been resolved to an *c.* 2 kb noncoding region that acts as a *cis*-regulatory element of *ZmRap2.7*, an AP2 transcription factor located *c.* 70 kb downstream (Salvi *et al.*, 2007). *ZmCCT9* (Huang *et al.*, 2018) and *ZmCCT10* (Ducrocq *et al.*, 2009; Hung *et al.*, 2012; Yang *et al.*, 2013) are two recently cloned CCT domain-containing proteins that confer long day-dependent flowering repression by negatively regulating the expression of *ZCN8*. Interestingly, two transposon insertions were identified in the upstream regulatory region of *ZmCCT9* and *ZmCCT10* and act in *cis* to repress the expression of *ZmCCT9* and *ZmCCT10* and, as a result, reduce photoperiod response under long-day conditions (Yang *et al.*, 2013; Huang *et al.*, 2018). These three loci are known to have played important roles during the adaptation of maize to higher latitudes (Ducrocq *et al.*, 2008; Yang *et al.*, 2013; Huang *et al.*, 2018).

In the present study, we report the identification and characterization of a flowering time QTL *qDTA3-2* that regulates the difference in flowering time between maize and teosinte. Through fine mapping, we resolved *qDTA3-2* to a MADS-box transcription factor, *ZmMADS69*. A transposon insertion mutant of *ZmMADS69* with reduced expression exhibits delayed flowering, while overexpression of *ZmMADS69* promotes flowering. We demonstrate that *ZmMADS69* functions as a constitutive flowering activator though the *ZmRap2.7-ZCN8* regulatory module. Population genetic analysis revealed that *ZmMADS69* was targeted by selection and might have played an important role in maize adaptation to temperate regions.

Materials and Methods

Materials

A large population of 866 maize-teosinte BC_2S_3 recombinant inbred lines (RILs) derived from a cross between W22, a typical temperate maize (*Zea mays* ssp. *mays*) inbred line, and CIMMYT accession 8759, a typical accession of teosinte (*Zea mays* ssp. *parviglumis*, hereafter referred to as 8759) was obtained from the Maize Genetics Cooperation Stock Center (Maize COOP). Detailed information regarding this BC_2S_3 RIL population has previously been reported (Hung *et al.*, 2012; Huang *et al.*, 2016, 2018; D. Li *et al.*, 2016; D. Y. Xu *et al.*, 2017; G. Xu *et al.*, 2017; Wang *et al.*, 2018). From a heterogeneous inbred family (HIF) that was heterozygous only at *qDTA3-2*, we developed two near-isogenic lines (NILs), one homozygous for W22 and one homozygous for 8759 across the *qDTA3-2* region, designated NIL(W22) and NIL(8759), respectively. NIL(W22) and NIL(8759) were planted in Tieling (42.1°N, 123.6°E), Liaoning province, China, during the summer of 2015 (the planting date was 8 May 2015) and in Sanya (18.4°N, 109.2°E), Hainan province, China, during the winter of 2015 (the planting date was 3 November 2015) to compare the difference in flowering time. NIL(W22) and NIL(8759) were scored for days to anthesis (DTA) and several other important agronomic traits (total leaf number, leaf number above the primary ear, leaf number below the primary ear, ear height, plant height, leaf width, leaf length, stem diameter, tassel branch length, tassel branch number, ear length and ear diameter).

Fine mapping of *qDTA3-2*

The fine-mapping strategy was the same as that employed in previous studies (Hung *et al.*, 2012; Huang *et al.*, 2016, 2018; D. Li *et al.*, 2016; D. Y. Xu *et al.*, 2017; G. Xu *et al.*, 2017). Two large F_2 populations derived from the HIF for *qDTA3-2* were successively used to identify recombinants to fine map *qDTA3-2*. A large F_2 population ($n = 3955$) was first planted in Tieling (42.1°N, 123.6°E), Liaoning province, China, during the summer of 2015 (the planting date was 8 May 2015). Recombinants were identified from the F_2 population using markers FM156440 and FM160558 that flank the support interval of *qDTA3-2*. To determine a general region of *qDTA3-2*, 20 recombinants were randomly selected (Supporting information Table S1) and their F_3 families were planted in Sanya (18.4°N, 109.2°E), Hainan province, China, during the winter of 2015 (the planting date was 3 November 2015). New markers were developed to further determine the recombination breakpoints of the F_2 recombinants. Within each recombinant-derived F_3 family, homozygous recombinant

(HR) and homozygous nonrecombinant (HNR) plants were identified using markers. The differences in flowering time between the HR and HNR plants within each family were determined using Student's *t*-test with the Bonferroni correction for multiple comparisons. If the HR and HNR plants exhibited a significant difference in flowering time, the parental F_2 recombinant was heterozygous for *qDTA3-2*; otherwise, the recombinant was homozygous for either parent. By integrating the QTL location information from all recombinants, *qDTA3-2* was initially delimited to a 476-kb physical region between markers FM158945 and FM159421. To further narrow down the region of *qDTA3-2*, another F_2 population ($n = 3266$) derived from the HIF was planted in Tieling (42.1°N, 123.6°E) during the summer of 2016 (the planting date was 6 May 2016). Recombinants between FM158945 and FM159421 were identified from the F_2 population (Table S2) and their F_3 families were planted in Sanya (18.4°N, 109.2°E) during the winter of 2016 (the planting date was 4 November 2016). *qDTA3-2* was finally localized to a 192-kb physical region between markers FM159020 and FM159212. The sequences of the markers used for fine mapping are listed in Table S3.

Expression analysis

To examine the spatiotemporal expression patterns of *ZmMADS69*, NIL(W22) and NIL(8759) were grown in Beijing (40.1°N, 116.2°E), China, during the summer of 2017 (the planting date was 11 May 2017). Various plant tissues, including root, stem, leaf sheath, mature leaves, immature leaves, SAM, developing tassel and ear, were collected from the two NILs at different development stages, with five biological replicates in each case. Total RNA was extracted using TRIzol (Invitrogen), treated with RNase-free DNase I (TaKaRa, Dalian, China) and purified using the RNAclean Kit (Tiangen, Beijing, China). The RNA samples were quantified using a NanoDrop ND-1000 spectrophotometer (Thermo Fisher Scientific, Waltham, MA, USA), and 2 μg of total RNA was reverse transcribed using a random primer and M-MLV reverse transcriptase (Promega) following the manufacturer's instructions. Quantitative real-time PCR (qRT-PCR) analysis was performed on an ABI 7500 instrument (Applied Biosystems Inc., Foster City, CA, USA) using the SYBR Premix Ex Taq II kit (Takara). The comparative C_T ($2^{-\Delta CT}$) method (Schmittgen & Livak, 2008) was used to quantify the *ZmMADS69* relative expression level. *ZmTubulin1* (GRMZM2G152466) was used as reference gene. The expression levels of *ZmRap2.7* and *ZCN8* were examined in the mature leaves of NIL(W22) and NIL(8759) collected at the floral transition stage. The transition from vegetative stage to flowering was judged by the extent of apex elongation and the appearance of branch meristems on the flanks of the SAM marking an early reproductive stage (Irish & Nelson, 1991). To validate the regulatory relationships among *ZmMADS69*, *ZmRap2.7* and *ZCN8*, a pair of NILs for *ZCN8* we previously developed were used, one homozygous for W22 and one homozygous for 8759 across the *ZCN8* region (Guo *et al.*, 2018). Mature leaves of NILs for *ZCN8* were harvested at the floral transition stage and the expression levels of *ZmMADS69* and *ZmRap2.7* were examined. The relevant primers used in qRT-PCR are listed in Table S3.

Subcellular localization

For subcellular localization in *Nicotiana benthamiana* leaf epidermal cells, the coding sequence of *ZmMADS69* without a stop codon was amplified from W22 cDNA and inserted into the pCUNm-eGFP plasmid to generate the Ubi::ZmMADS69-eGFP fusion protein. *Agrobacterium tumefaciens* containing the plasmid was resuspended in infiltration buffer and infiltrated into 5-wk-old leaves of *N. benthamiana*. After infiltration, plants were placed at 24°C for 60 h. To further verify the subcellular localization, the construct was also transformed into maize leaf protoplasts using polyethylene glycol (PEG)-mediated transformation as previously described (Yoo *et al.*, 2007). Mesophyll protoplasts were isolated from the leaves of 12-d-old etiolated B73 seedlings following a previously described method (Yoo *et al.*, 2007). The protoplasts were cultured at 25°C in the dark for 18 h, and GFP fluorescence was observed via confocal microscopy using a Zeiss 710 microscope (Carl Zeiss, Oberkochen, Germany).

Transgenic functional validation

The coding sequence of *ZmMADS69* was amplified from W22 cDNA and cloned into the binary vector pCUNm-eGFP under control of the *Ubiquitin* promoter. This construct was introduced into the receptor line B73 via *Agrobacterium tumefaciens*-mediated transformation (Ishida *et al.*, 2007). Three independent T0 transgenic plants (OE#1, OE#2 and OE#3) were self-pollinated to generate progenies for phenotypic testing. T1 families from these three T0 plants were planted in Sanya (18.4°N, 109.2°E) during the winter of 2017 (the planting date was 8 November 2017). Transgene-positive and transgene-negative plants were identified in T1 families using transgene-specific primers (Table S3). Mature leaves of T1 plants were collected at the floral transition stage for the expression analysis of *ZmMADS69, ZmRap2.7* and *ZCN8* via qRT-PCR. Due to the limited number of T2 seeds of OE#3, it was only possible to plant the OE#1 and OE#2 T2 families in a greenhouse (14 h : 10 h, light : dark) to examine flowering time. The T1 and T2 families were scored for DTA, leaf number, ear height, plant height, leaf length, leaf width, stem diameter, tassel branch number, tassel branch length, ear length and ear diameter. Phenotypic differences between transgene-positive and transgene-negative plants were determined using Student's *t*-test.

Mutant functional validation

The position of the *Mu* insertion in *ZmMADS69* (UFMu-01868) was confirmed using a combination of primers designed to anneal to the Mu-TIR sequence and genic sequences near the putative *Mu* insertion. Homozygous *Mu* insertion mutants were

crossed to the wildtype W22 and the resulting heterozygous progeny were backcrossed to a plant homozygous for the *Mu* insertion to generate 1 : 1 segregating families. Segregating families were planted near Ames (42.0°N, 93.8°W) and Boone (42.0°N, 93.7°W), Iowa, during the summer of 2017 (the planting dates were 9 May 2017 and 26 May 2017, respectively) and were scored for DTA and ear height. Phenotypic differences were tested using Student's *t*-test. Mature leaves of *ZmMADS69* homozygous mutant and heterozygous siblings were sampled at the floral transition stage with three biological replicates in each case. RNA was extracted using the RNeasy Plant mini kit (Qiagen, Hilden, Germany) according to the manufacturer's manual. The comparative C_T ($2^{-\Delta CT}$) method (Schmittgen & Livak, 2008) was used to quantify gene relative expression level. *ZmTubulin1* (GRMZM2G152466) was used as reference gene.

Generation and analysis of CRISPR/Cas9 knockout lines of *ZmRap2.7* and *ZCN8*

Two 20-bp target sequences in the coding regions of *ZmRap2.7* and *ZCN8* were selected for Cas9 cleavage. The CRISPR/Cas9 knockout vector was constructed according to previously described protocol (Xing *et al.*, 2014; Huang *et al.*, 2018). The resulting vector was confirmed by sequencing and introduced into the receptor line B73 via *Agrobacterium tumefaciens*-mediated transformation (Ishida *et al.*, 2007). Sequencing analysis of *ZmRap2.7* and *ZCN8* T0 transgenic plants identified one transgenic line carrying homozygous deletions at the target sites that resulted in frame shift of the *ZmRap2.7* ORF and two transgenic lines carrying homozygous deletions at the target sites that resulted in the loss of the PEBP domain of ZCN8 protein. T1 progenies of *ZmRap2.7* and *ZCN8* T0 transgenic plants were planted under long days and scored for flowering time. Mature leaves of T1 and wildtype plants (nontransgene plants) were sampled at the floral transition stage with four biological replicates in each case for gene expression analysis.

RNA sequencing and differential gene expression analysis

The *ZmMADS69* transgenic line OE#2 was used for RNA sequencing. In the T1 family derived from OE#2, three transgene-positive and three transgene-negative plants were randomly selected, and the mature leaves were collected at the floral transition stage. Total RNA extraction and purification were performed as described above. Total RNA quality was verified using an Agilent 2100 Bioanalyzer (Agilent Technologies, Santa Clara, CA, USA). mRNA libraries were prepared from *c.* 5 μg of total RNA and sequenced using a HiSeq 150-bp paired-end Illumina RNA-seq protocol. Sequencing reads (accession number PRJNA491787) were first processed with Trimmomatic (Bolger *et al.*, 2014) to remove low-quality bases at the 5′ and 3′ ends ($q < 20$), and reads > 75 bp were kept for subsequent analysis. The high-quality reads were then aligned to the B73 reference sequence v3 (AGPv3) (Schnable *et al.*, 2009) using HISAT2 (Pertea *et al.*, 2016), with a minimum intron size of 60 bp and a maximum intron size of 50 000 bp. Only uniquely mapped reads were kept for subsequent gene expression quantification using HTSeq-count (Anders *et al.*, 2015), with the intersection-strict option. To evaluate the repeatability of biological replicates, hierarchical clustering and multidimensional scaling (MDS) analysis were performed using R function HCLUST and ISOMDS (https://www.r-project.org/), respectively. Differential gene expression analysis between transgene-positive and transgene-negative plants was performed using the EDGER package (Robinson *et al.*, 2010), which employs a robust negative binominal distribution to account for the biological variation and dispersion from all genes (Rapaport *et al.*, 2013). The *P*-value of differential expression was determined using the exact test and was corrected with Benjamin and Hochberg's algorithm (Benjamini & Hochberg, 1995). Expression was considered to be significantly different at a threshold of false discovery rate (FDR) ≤ 0.01 and fold change ≥ 2.

Nucleotide diversity analysis and selection test

The third-generation *Zea mays* haplotype map (HapMap 3) data was downloaded from https://www.panzea.org/ (Bukowski *et al.*, 2018) and was used to examine the nucleotide diversity along the 192-kb causative region for *qDTA3-2* in maize and teosinte. The R package POPGENOME (Pfeifer *et al.*, 2014) was used for population genomic analysis. Sliding windows (window size = 1000 bp, step size = 100 bp) across the 192-kb causative region were generated using the function sliding.window.transform. Nucleotide diversity (π) in each sliding window was calculated for maize and teosinte using the function diversity.stats. At the same time, we resequenced seven fragments (accession numbers MH937291–MH937329 and MH988461–MH988687) from the *ZmMADS69* gene amplified from a diverse panel of 28 maize inbred lines and 17 teosinte accessions (*Zea mays* ssp. *parviglumis*) (Table S4). Because the first intron of *ZmMADS69* is 23.5-kb long, two fragments were selected from this intron for sequencing. The 28 diverse maize inbred lines include the 26 founder lines of the maize NAM population, the Mo17 founder of the B73 × Mo17 (IBM) population and the W22 parent of our maize-teosinte BC_2S_3 population and the genetic background of our *Mu* insertion allele (Table S4). Sequencing reactions were performed in both directions. Multiple sequence alignments were performed using BIOEDIT v.7.1.3.0 (Hall, 1999) and manually edited when necessary. Nucleotide diversity was calculated using DNASP v.5.10.00 (Librado & Rozas, 2009). Insertions and deletions were not included in the analysis. The retention of the nucleotide diversity, which is the relative ratio of π in maize to π in teosinte, was calculated in each sequenced region. Following a previously described procedure (Tian *et al.*, 2009; G. Xu *et al.*, 2017; Huang *et al.*, 2018), coalescent simulations incorporating the domestication bottleneck (Eyre-Walker *et al.*, 1998; Tenaillon *et al.*, 2004) were performed to evaluate whether the observed loss of nucleotide diversity in maize relative to that in teosinte could be explained by a domestication bottleneck alone using Hudson's MS program (Hudson, 2002). All parameters in the model were assigned to previously established values (Wright *et al.*, 2005;

Tian *et al.*, 2009; G. Xu *et al.*, 2017; Huang *et al.*, 2018). The population mutation and population recombination parameters were estimated from the teosinte sequences. In total, 10 000 coalescent simulations were performed.

Results and Discussion

qDTA3-2 regulates the difference in flowering time between maize and teosinte

To identify genetic factors controlling the difference in flowering time between maize and teosinte, we previously performed QTL mapping for DTA in the 866 maize-teosinte BC_2S_3 RIL population (D. Li *et al.*, 2016). Among the mapped loci, a significant flowering time QTL, *qDTA3-2*, was detected between markers M16870 and M16969 on chromosome 3 (Figs 1a, 2a). The lines homozygous for the teosinte allele at *qDTA3-2* flowered *c.* 2.5 d later than the lines homozygous for the maize allele under natural long days (Beijing, 40.1°N, 116.2°E) (Fig. 1b). Interestingly, previous genetic mapping studies using different populations also detected significant flowering time QTLs at similar regions (Buckler *et al.*, 2009; Salvi *et al.*, 2011), indicating the importance of the region around *qDTA3-2* in regulating the natural variation in flowering time in maize. However, at the mapping resolutions of these QTL studies, it is difficult to tell whether these detected QTLs reflect the action of a single causative gene or alternatively several closely linked QTLs, with each having causative polymorphisms in different genes.

To further evaluate the phenotypic effects of *qDTA3-2*, we planted the two NILs for *qDTA3-2*, NIL(W22) and NIL(8759), under natural long days (Tieling, 42.1°N, 123.6°E) and short days (Sanya, 18.4°N, 109.2°E) and compared their phenotypic differences. Under both long days and short days, the two NILs exhibited a similar flowering time difference, with NIL(W22) flowering *c.* 2 d earlier than NIL(8759) (Fig. 1c). These results indicate that *qDTA3-2* is insensitive to differences in day length. In addition to flowering time, NIL(W22) and NIL(8759) also exhibited significant differences in plant height, ear height, leaf number, leaf length, tassel branch number, tassel branch length, ear length and ear diameter (Figs 1d, S1), suggesting that *qDTA3-2* might be pleiotropic for many traits of agronomic importance.

Fine mapping of *qDTA3-2*

To identify the gene underlying *qDTA3-2*, we performed fine mapping following a previously described method (Hung *et al.*, 2012; D. Li *et al.*, 2016; Huang *et al.*, 2018). A large F_2 population ($n = 3955$) was generated by self-pollinating the HIF for *qDTA3-2*, and recombinants were identified from the F_2 population using markers FM156440 and FM160558 that flank the target region. To determine the general region in which *qDTA3-2* resides, 20 F_2 recombinants were randomly selected, and their F_3 families were planted in the field for genotypic and phenotypic analyses (Table S1). Within each recombinant-derived F_3 family, HRs and HNRs were identified using markers, and their differences in flowering time were compared to determine the genotype of *qDTA3-2* in the parental recombinant. By integrating the QTL location information from all recombinants, *qDTA3-2* was delimited to a 476-kb physical region between markers FM158945 and FM159421 (Fig. 2a; Table S1). To further fine map *qDTA3-2*, another F_2 population ($n = 3266$) was generated, and the recombinants between markers FM158945 and FM159421 were identified. In total,

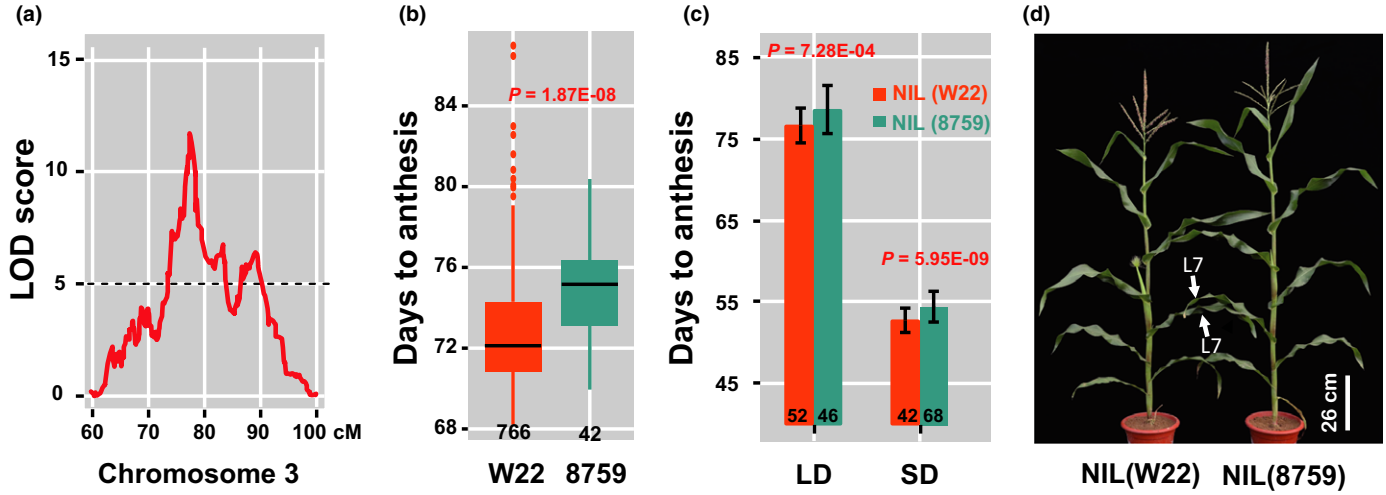

Fig. 1 *qDTA3-2* regulates maize flowering. (a) Logarithm of odds (LOD) plots of flowering time quantitative trait loci (QTL), *qDTA3-2*. The black horizontal line represents the $P < 0.05$. LOD significance threshold as determined by a permutation test. (b) Phenotypic differences in days to anthesis (DTA) under natural long-day (LD) conditions (Beijing, 40.1°N, 116.2°E) between recombinant inbred lines (RILs) from the maize-teosinte BC_2S_3 RIL population carrying contrasting alleles of *qDTA3-2*. The numbers below the boxplots indicate the numbers of RILs carrying W22 and 8759 alleles. (c) Phenotypic differences in DTA under natural LD and short-day (SD) conditions between NIL(W22) and NIL(8759) for *qDTA3-2*. Reported values represent the mean ± standard deviation; *P*-values were determined using Student's *t*-test: **, $P < 0.01$. The numbers on the bars indicate the numbers of plants scored in each near-isogenic line (NIL). (d) Gross morphologies of NIL(W22) and NIL(8759). The seventh leaf on each plant is indicated by a white arrow.

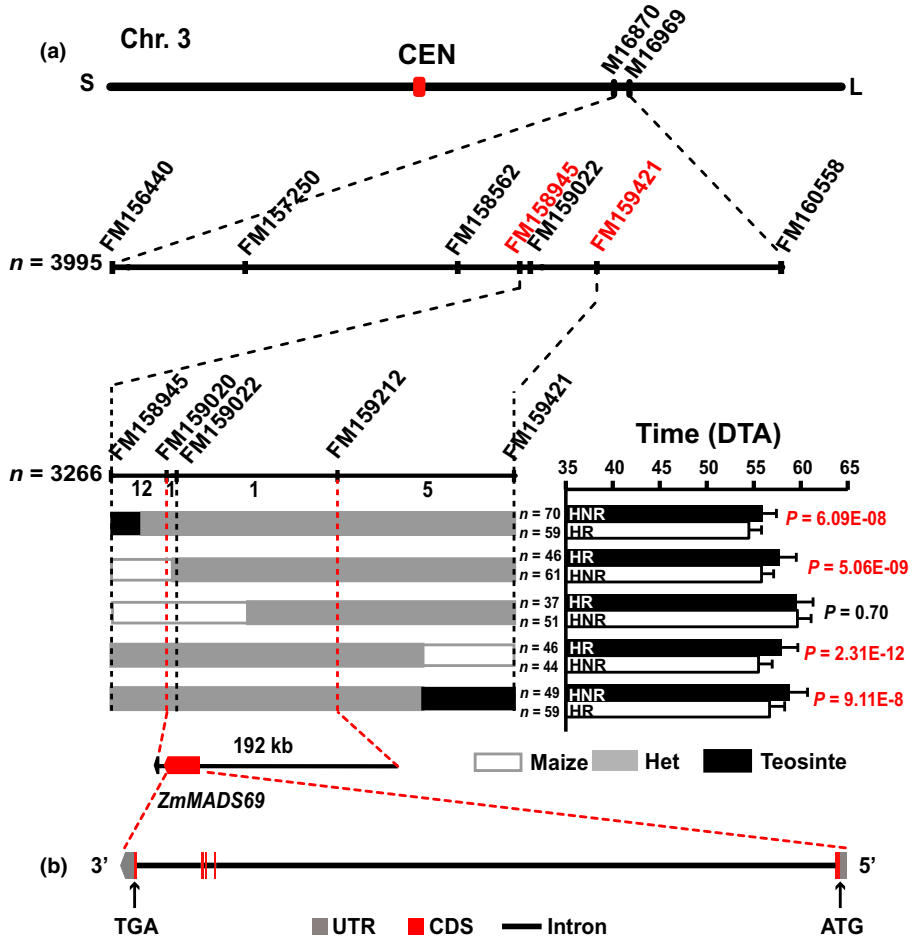

Fig. 2 Fine mapping of *qDTA3-2*. (a) Chromosomal location and fine mapping of flowering time quantitative trait loci (QTL), *qDTA3-2*. Two large F_2 populations were used to identify recombinants for fine mapping of *qDTA3-2*. The numbers of recombinants between adjacent markers used for fine mapping are indicated below the linkage map. Progeny testing of recombinants finally narrowed the *qDTA3-2* locus to a 192-kb physical region between markers FM159020 and FM159212. The lower panel shows the graphical genotypes of five representative recombinants. White and black boxes indicate chromosomal regions homozygous for the maize and teosinte haplotypes, respectively. Gray boxes represent heterozygous chromosomal regions. The bar graphs on the right compare the days to anthesis (DTA) between homozygous recombinants (HR) and homozygous nonrecombinants (HNR) within each recombinant-derived F_3 family (see the Materials and Methods section). Reported values represent the mean ± standard deviation. *P*-values were determined using Student's *t*-test. CEN, centromere. The red box in the 192-kb fine-mapping region indicates the *ZmMADS69* gene, with the arrow showing the direction of transcription. (b) Gene structure of *ZmMADS69*. Gray boxes represent the 5′ and 3′ UTRs, red boxes represent coding sequence region, while black lines represent introns. ATG and TGA indicate the start and stop codons, respectively.

19 recombinant-derived F_3 families (Table S2) were used to further narrow down the region of *qDTA3-2*. *qDTA3-2* was finally localized to a 192-kb physical region between markers FM159020 and FM159212 (Fig. 2a; Table S2).

According to the B73 reference genome (AGPv3), the 192-kb region contains 400-bp of GRMZM2G171622 and one intact gene, GRMZM2G171650 (Fig. 2b). GRMZM2G171622 encodes a CBS domain-containing protein. Studies in *Arabidopsis* and rice have shown that CBS domain-containing proteins were involved in biotic or abiotic stress response (Kushwaha *et al.*, 2009; Singh *et al.*, 2012; Mou *et al.*, 2015; Kumar *et al.*, 2018). GRMZM2G171650 encodes a MADS-box transcription factor designated *ZmMADS69* (which has also been termed *zmm22*) in the MaizeGDB database (https://www.maizegdb.org/). MADS-box transcription factors are known to play important roles in plant inflorescence and flower development (Smaczniak *et al.*, 2012). Previously, we used eRD-GWAS, which employs gene expression levels, rather than SNPs as explanatory variables in GWAS to identify 26 genes, including *ZmMADS69* that are associated with DTA (Lin *et al.*, 2017). Hence, *ZmMADS69* was the most likely candidate gene underlying *qDTA3-2*.

ZmMADS69 underlies *qDTA3-2*

ZmMADS69 contains five exons and encodes a 166-amino-acid protein (Figs 2b, S2). Interestingly, a comparison of the *ZmMADS69* coding sequence (CDS) between W22 and 8759 revealed no sequence variants in the protein-coding region (Fig. S2), suggesting that *ZmMADS69* might exhibit expression differences between the parental alleles. To test this hypothesis, we investigated the spatiotemporal expression patterns of

ZmMADS69 in NIL(W22) and NIL(8759). *ZmMADS69* was broadly expressed in various tissues including root, stem, leaf sheath, mature leaf, immature leaf, SAM, developing tassel and ear (Fig. 3a). *ZmMADS69* exhibited higher expression in the early-flowering NIL(W22) than in the late-flowering NIL(8759) in all examined tissues, with the maximum expression observed in mature leaves sampled at the floral transition stage (Fig. 3a). To further determine whether the difference in the expression of *ZmMADS69* detected between the parents of the maize-teosinte population is common in maize natural populations, we analyzed the recently published transcriptome data of the leaf tissues of 265 diverse maize inbred lines (Kremling *et al.*, 2018). Consistent with the results from NILs and the results from our previously reported eRD-GWAS, increased expression of *ZmMADS69* was significantly associated with earlier flowering in natural populations (Fig. S3). A similar observation has been reported by Hirsch *et al.* (2014) who used another association panel of 503 diverse inbred lines. These results strongly suggested that regulatory variation in *ZmMADS69* might contribute to natural variation in flowering time in maize. We are using larger segregating populations to further delimit the region of *qDTA3-2* to identify the causative variant(s).

We used two independent approaches to test the hypothesis that *ZmMADS69* regulates flowering time. First, we overexpressed *ZmMADS69* under the control of the *Ubiquitin* promoter. This promoter was selected because *ZmMADS69* is broadly expressed in various tissues (Fig. 3a). Second, we analyzed a *Mu* transposon insertion mutant (UFMu-01868) of *ZmMADS69* isolated from the UniformMu reverse genetics resource (McCarty *et al.*, 2005; Settles *et al.*, 2007). Three independent T0 transgenic lines (OE#1, OE#2 and OE#3) carrying the overexpression construct were obtained. T1 families from OE#1, OE#2 and OE#3 were planted under natural short days (Sanya, 18.4°N, 109.2°E) to investigate flowering time. The results showed that transgene-positive plants with higher *ZmMADS69* expression flowered 5–8 d earlier than transgene-negative plants in the three T1 families (Fig. 4a–c). We further planted T2 families of *ZmMADS69* overexpressed lines in a greenhouse under long-day conditions where we observed that *ZmMADS69* overexpressed lines flowered significantly earlier than wildtype controls (Fig. S4). These results, together with the phenotypic analyses of NILs for *qDTA3-2* under long days and short days, consistently indicated that *ZmMADS69* is a constitutive flowering activator that is insensitive to differences in day length. In addition to flowering time, *ZmMADS69* overexpressed plants also exhibited significant phenotypic effects in many other important agronomic traits, including reduced plant height, ear height, leaf number, stem diameter, tassel and ear size as compared with wild type (Figs S4, S5). These phenotypic effects were consistent with phenotypic analyses in the two NILs for *qDTA3-2*.

In parallel, using PCR and sequencing, we confirmed that an allele isolated from the UniformMu collection contains a *Mu* transposon insertion in the first intron of *ZmMADS69* (UFMu-01868), which downregulated the expression of *ZmMADS69* (Fig. 4d,e). DTA was measured within a population segregating

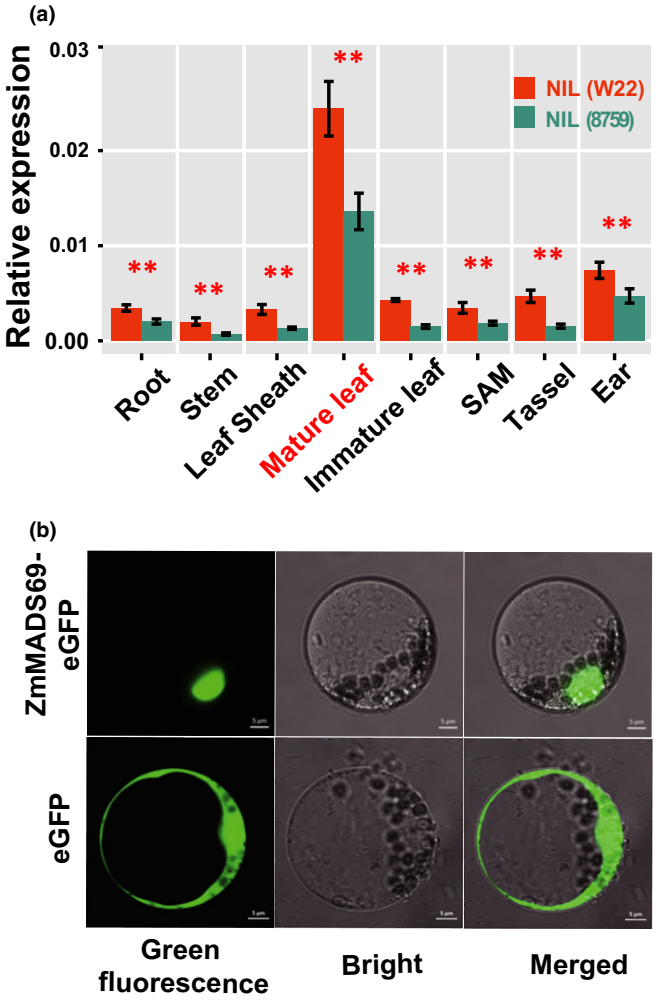

Fig. 3 Expression patterns and subcellular localization of *ZmMADS69*. (a) The expression patterns of *ZmMADS69* in NIL(W22) and NIL(8759) across tissues/organs. Reported values represent the mean ± standard deviation; *P*-values were determined using Student's *t*-test: **, $P < 0.01$. (b) The ZmMADS69 protein localizes to the nucleus in maize protoplasts (bars, 5 μm). A Ubi::ZmMADS69-GFP fusion construct driven by *Ubiquitin* promoter was used to assess protein localization (upper panel); Ubi::GFP was used as a control (lower panel). Green fluorescence (left), bright (middle), and overlay (right) images of maize protoplast cell were shown, respectively.

1 : 1 for siblings homozygous or heterozygous for the insertion allele grown at two Iowa locations during the summer of 2017. As shown in Figs 4f and S6, homozygous mutant plants flowered *c.* 3 d later than heterozygous siblings and were *c.* 7 cm taller.

Together the analyses of overexpression and *Mu* insertion alleles demonstrate that *ZmMADS69* functions as a flowering activator and that this gene also has pleiotropic effects on multiple other agronomic traits.

ZmMADS69 functions through the *ZmRap2.7-ZCN8* regulatory module

To determine the subcellular localization of the ZmMADS69 protein, a fusion protein containing ZmMADS69 and enhanced green fluorescent protein (eGFP) under the control of the *Ubiquitin* promoter (Ubi::ZmMADS69−eGFP) was constructed

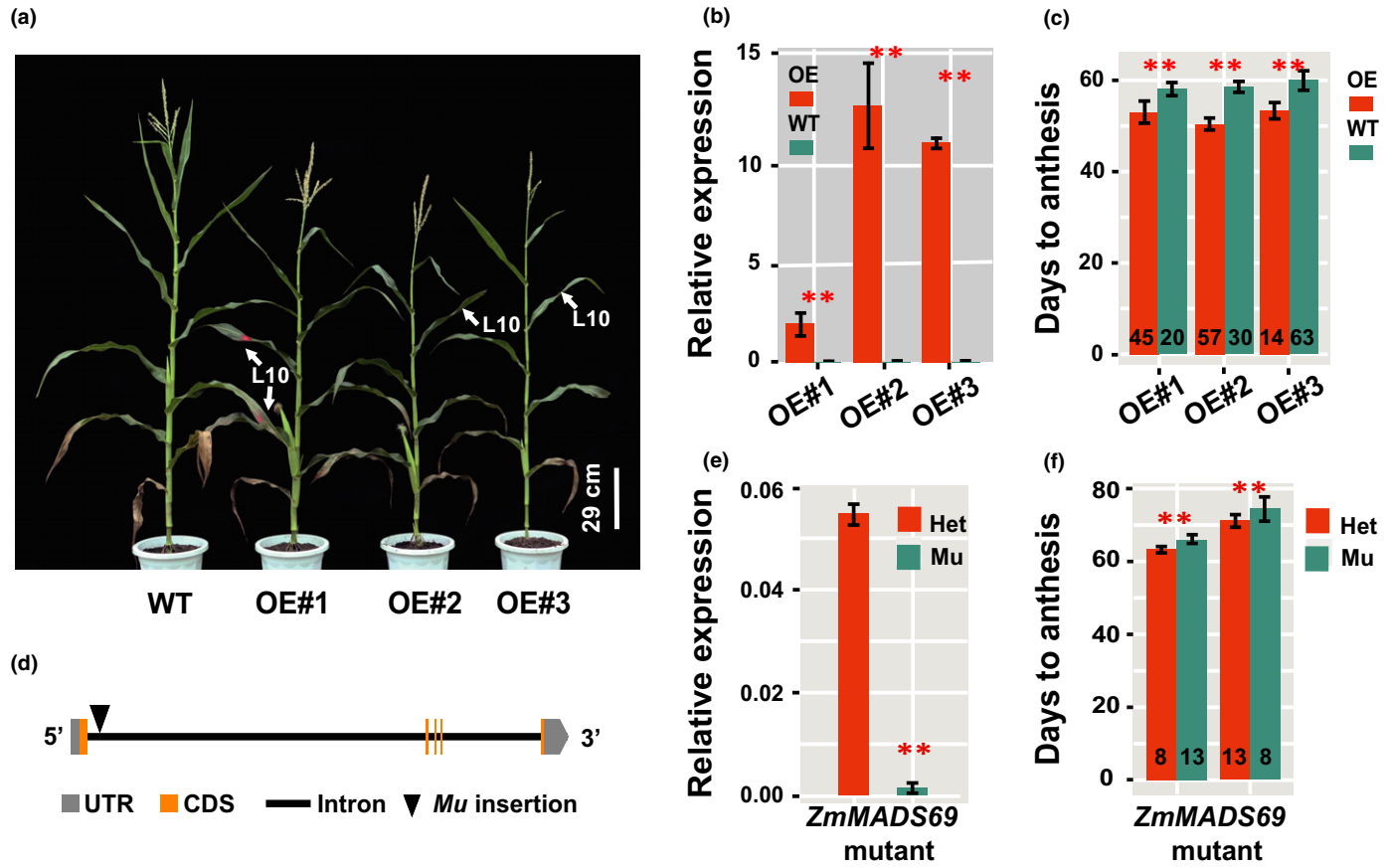

Fig. 4 Functional validation of *ZmMADS69*. (a) Gross morphologies of wildtype (WT) and three overexpression lines (OE#1, OE#2 and OE#3). The 10th leaf on each plant is indicated by a white arrow. (b) *ZmMADS69* expression levels in T_1 transgenic families. In each T_1 family, transgene-positive plants (OE, $n = 4$) and transgene-negative (WT, $n = 4$) plants were randomly selected for expression assays. (c) Days to anthesis (DTA) of *ZmMADS69* transgene-positive (OE) and transgene-negative (WT) plants. (d) *ZmMADS69* mutant containing a *Mu* transposon insertion in the first intron of *ZmMADS69*. Gray boxes represent the 5′ and 3′ UTRs, orange boxes represent coding sequence region, while black lines represent introns. (e) *ZmMADS69* expression levels in the mature leaves of homozygous mutants ($n = 3$) and heterozygous siblings ($n = 3$). (f) DTA of homozygous mutants and heterozygous siblings grown near Ames and Boone, Iowa. Reported values represent the mean ± standard deviation; *P*-values were determined using Student's *t*-test: **, $P < 0.01$ (b, c, e, f).

and introduced into epidermal cells of *Nicotiana benthamiana* leaves and maize protoplasts. GFP fluorescence was localized to the nucleus (Figs 3b, S7), supporting a role for *ZmMADS69* as a nuclear transcription factor.

To understand the function of *ZmMADS69* in the maize flowering pathway, we sequenced the transcriptomes of mature leaves from *ZmMADS69* transgene-positive and negative plants derived from OE#2 (Figs S8, S9). A total of 2292 genes exhibited significant expression differences between *ZmMADS69* transgene-positive and negative plants (fold change ≥ 2, FDR < 0.01; Fig. 5a; Table S5). Interestingly, several known maize flowering genes, including *ZmRap2.7* and *ZCN8*, were among the differentially expressed genes (Fig. 5a; Table S5), and their expression differences were validated by qRT-PCR analysis (Fig. 5b).

ZCN8, which encodes florigen and is required for floral induction in maize (Lazakis *et al.*, 2011; Meng *et al.*, 2011), was significantly upregulated in *ZmMADS69* overexpressed plants compared with the level in *ZmMADS69* transgene-negative plants (Fig. 5a,b). We further examined *ZCN8* expression in the two NILs for *qDTA3-2*. Consistent with the RNA-seq results, NIL(W22), which flowered significantly earlier than NIL(8759), exhibited higher *ZCN8* expression (Fig. 5c). *ZmRap2.7* is an AP2 transcription factor that functions as a flowering repressor in maize (Salvi *et al.*, 2007; Dong *et al.*, 2012). We found that *ZmRap2.7* expression was significantly downregulated in plants overexpressing *ZmMADS69* (Fig. 5a,b). Consistent with this result, NIL(W22) exhibited lower expression of *ZmRap2.7* than NIL(8759) (Fig. 5c). Taken together, these results indicate that *ZmMADS69* functions upstream of *ZCN8* and *ZmRap2.7*.

To further determine the regulatory relationships among *ZmMADS69*, *ZmRap2.7* and *ZCN8*, we produced knockout lines for *ZmRap2.7* and *ZCN8* using CRISPR/Cas9 (Doudna & Charpentier, 2014; Belhaj *et al.*, 2015) (Figs S10, S11). Compared with wildtype plants, *ZmRap2.7* knockout plants flowered *c.* 2.6 d earlier (Fig. S12), whereas *ZCN8* knockout plants flowered *c.* 12 d later (Fig. S13), results which are consistent with previously published findings on the functions of *ZmRap2.7* and *ZCN8* (Salvi *et al.*, 2007; Meng *et al.*, 2011). We examined the expression levels of *ZmMADS69*, *ZmRap2.7* and *ZCN8* in the *ZmRap2.7* and *ZCN8* knockout lines. *ZCN8* expression was

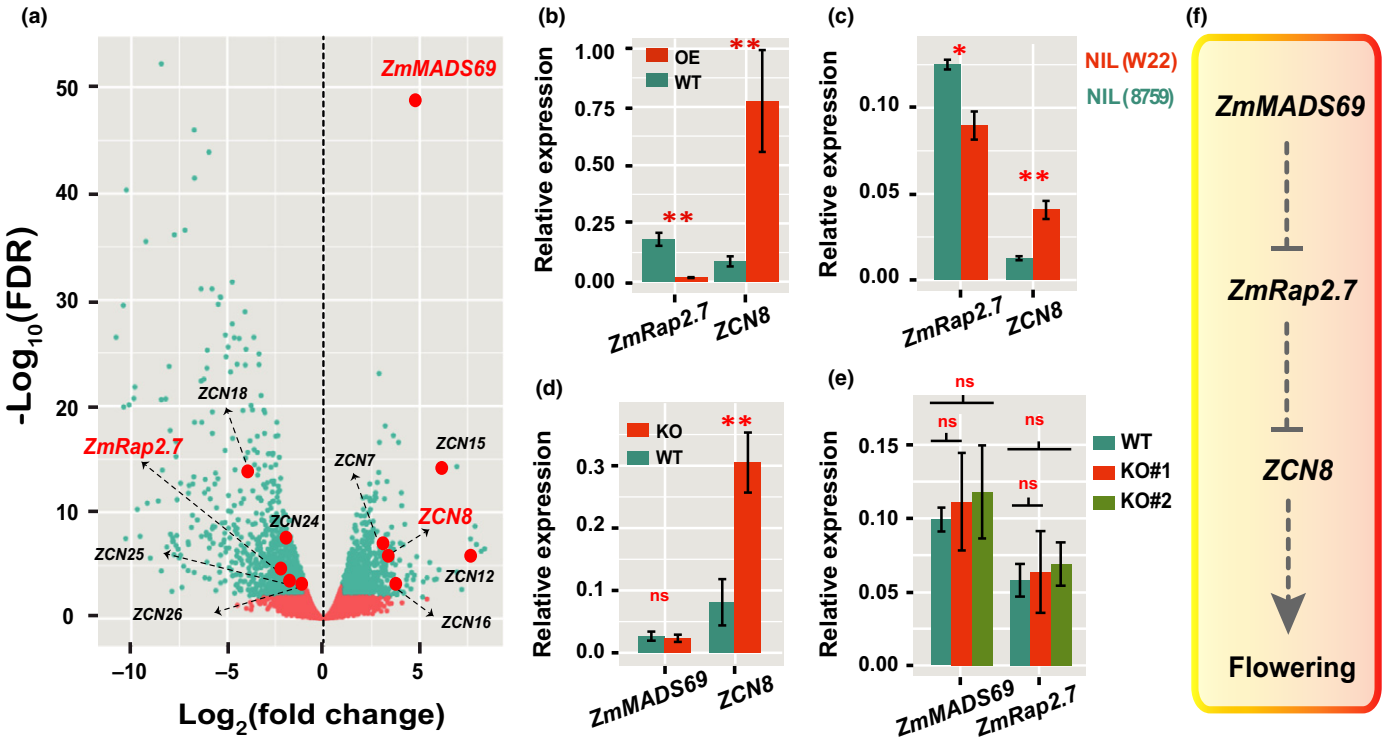

Fig. 5 *ZmMADS69* functions through the *ZmRap2.7-ZCN8* regulatory module. (a) Volcano plot of significantly differentially expressed genes between *ZmMADS69* transgene-positive and transgene-negative plants. Positive and negative values on the *x*-axis indicate upregulated and downregulated genes, respectively, in *ZmMADS69* transgene-positive plants compared with transgene-negative plants. The light blue points represent differentially expressed genes (false discovery rate (FDR) < 0.01, fold change ≥ 2). (b) Quantitative real-time PCR (qRT-PCR) assay of *ZmRap2.7* and *ZCN8* expression levels in mature leaves of *ZmMADS69* transgene-positive ($n = 4$) and transgene-negative plants ($n = 4$) derived from OE#2. (c) Expression levels of *ZmRap2.7* and *ZCN8* in mature leaves of near-isogenic lines (NILs) carrying contrasting alleles of *qDTA3-2* ($n = 5$). (d) Expression levels of *ZmMADS69* and *ZCN8* in *ZmRap2.7* knockout line ($n = 3$) and nontransgene wildtype (WT, $n = 3$). (e) The expression levels of *ZmMADS69* and *ZmRap2.7* in *ZCN8* knockout lines ($n = 4$) and nontransgene WT ($n = 4$) control. (f) Proposed model for the function of *ZmMADS69* in the maize flowering pathway. Reported values represent the mean ± standard deviation; *P*-values were determined using Student's *t*-test: **, $P < 0.01$; *, $P < 0.05$; ns, not significant (b–e).

significantly upregulated in *ZmRap2.7* knockout plants compared with wildtype plants (Fig. 5d). However, the expression of *ZmMADS69* was not altered in these plants (Fig. 5d). Hence, these results suggested that *ZmRap2.7* functions downstream of *ZmMADS69* but upstream of *ZCN8*. The *ZmMADS69* and *ZmRap2.7* genes exhibited similar expression levels in *ZCN8* knockout and wild-type plants (Fig. 5e). Additionally, we also examined *ZmMADS69* and *ZmRap2.7* expression in the two NILs for *ZCN8* (Guo *et al.*, 2018) and no significant differences in expression were observed between the two NILs (Fig. S14). These results indicated that *ZCN8* functions downstream of *ZmRap2.7* and *ZmMADS69*. Given these results, we propose the *ZmMADS69-ZmRap2.7-ZCN8* regulatory module, wherein *ZmMADS69* represses *ZmRap2.7* expression, which in turn relieves the repression of *ZCN8* and, as a result, promotes flowering (Fig. 5f). However, the possibility of *ZmMADS69* functioning in other pathways cannot be excluded given its broad expression across various tissues and significant impact on the expression of numerous genes.

Interestingly, aside from *ZCN8*, the expression levels of eight additional *FT*-like genes, including *ZCN7*, *ZCN12*, *ZCN15*, *ZCN16*, *ZCN18*, *ZCN24*, *ZCN25* and *ZCN26*, were also significantly altered in plants overexpressing *ZmMADS69* (Fig. 5a; Table S5). It has been shown that *ZCN7*, a *ZCN8* paralog, might be a second maize florigen gene (Mascheretti *et al.*, 2015). Recently, Minow *et al.* (2018) reported that six *FT*-like genes, including *ZCN7*, *ZCN8*, *ZCN12*, *ZCN15*, *ZCN18* and *ZCN26*, were also differentially expressed at the floral transition stage in mature teosinte leaves between inductive short-day conditions and noninductive night-break conditions (Minow *et al.*, 2018). These results suggest that these *FT*-like genes may play important roles in mediating maize flowering. However, their specific roles need to be elucidated.

ZmMADS69-ZmRap2.7-ZCN8 contributes to maize flowering time adaptation

From its tropical origin in southwestern Mexico, maize has expanded broadly into temperate zones, a process which required flowering time adaptation. Given its regulatory importance in flowering time, we speculated that the *ZmMADS69-ZmRap2.7-ZCN8* regulatory module might have been targeted by selection as maize spread to higher latitudes. A miniature transposon (MITE) located *c.* 70-kb upstream of *ZmRap2.7* is the causative variant of *Vgt1*, a major maize flowering time QTL (Salvi *et al.*, 2007; Castelletti *et al.*,

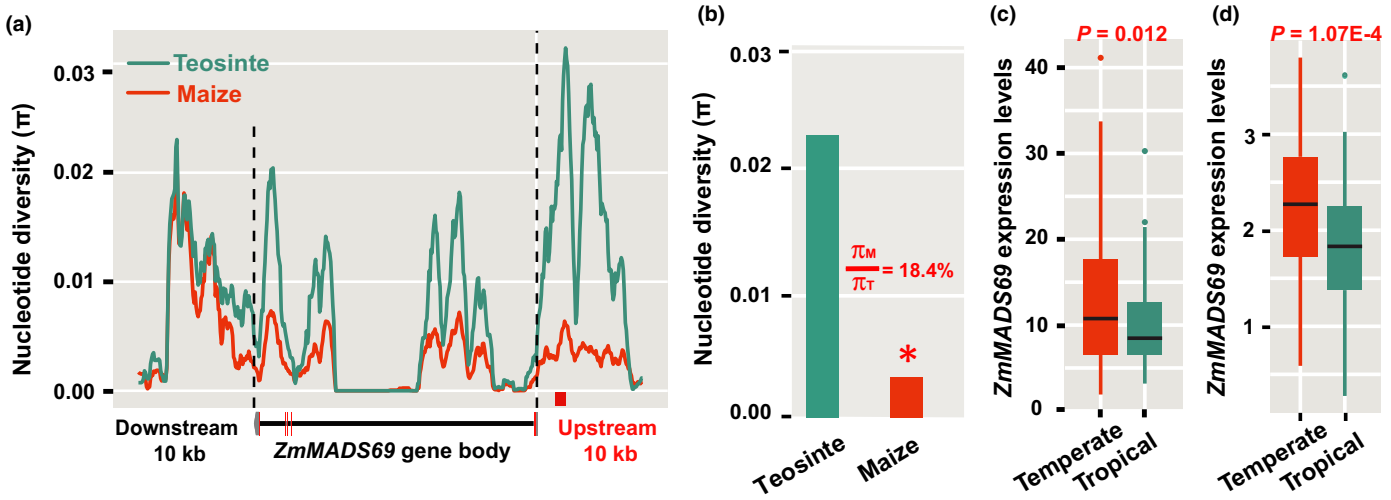

Fig. 6 Evidence of selection at *ZmMADS69*. (a) Analysis of HapMap 3 data revealed that the 5′ regulatory region of *ZmMADS69* exhibited very low nucleotide diversity (π) in maize relative to teosinte. The green and orange curves represent the nucleotide diversity of teosinte and maize surrounding *ZmMADS69*, respectively. The red box on *x*-axis indicates the resequenced region in diverse maize and teosinte lines. (b) Resequencing analysis and coalescence simulations validated that the 5′ regulatory region of *ZmMADS69* was targeted by selection. *P*-values were determined using coalescence simulations: *, $P < 0.05$. (c, d) Comparison of *ZmMADS69* expression levels between tropical and temperate inbred lines in the apex based on data from Lin *et al.* (2017) (c), and the tip of the third leaf based on data from Kremling *et al.* (2018) (d).

2014). The frequency of this MITE insertion exhibited a strong correlation with elevation and latitude, indicating a key role of *Vgt1* in maize alti-latitudinal adaptation (Ducrocq *et al.*, 2008). We recently showed that two natural *cis*-variants in the promoter of *ZCN8* were targeted by selection in a stepwise manner and played distinct roles as maize spread from its tropical origin to temperate zones (Guo *et al.*, 2018). To determine whether *ZmMADS69* was also a target of selection, we analyzed the nucleotide diversity around *ZmMADS69* using the third-generation *Zea mays* haplotype map (HapMap 3) containing ultra-high-density SNPs across maize genome (Bukowski *et al.*, 2018). Notably, the promoter region of *ZmMADS69* exhibited obvious reduction of nucleotide diversity in maize as compared with teosinte (Fig. 6a). To further verify this result, we resequenced six fragments across the gene body region of *ZmMADS69* and one *c.* 1-kb fragment from the promoter region of *ZmMADS69* in a diverse panel of 28 maize inbred lines and 17 teosinte accessions (*Zea mays* ssp. *parviglumis*) (Fig. S15; Table S4). Because the first intron of *ZmMADS69* is 23.5-kb long, two portions of it were selected for sequencing. We calculated the amount of nucleotide diversity retained in maize relative to teosinte in each sequenced region. Across the six fragments in the gene body of *ZmMADS69*, maize on average retained 47–73% of the nucleotide diversity of teosinte. By contrast, in the sequenced promoter fragment, maize retained only 18.4% of the nucleotide diversity of teosinte (Figs 6b, S15). Coalescent simulations that incorporate the domestication bottleneck (Eyre-Walker *et al.*, 1998; Tian *et al.*, 2009) detected a significant deviation from expectation under a neutral domestication bottleneck for the promoter fragment (Figs 6b, S15), indicating that the 5′ regulatory region of *ZmMADS69* was affected by selection. Because increasing *ZmMADS69* expression promotes flowering, the selection at the 5′ regulatory region may cause upregulation of *ZmMADS69* expression as maize spread into temperate environments. To test this hypothesis, we analyzed the expression difference between temperate and tropical maize inbred lines from our association panel. Consistent with our hypothesis, temperate lines exhibited higher *ZmMADS69* expression than tropical lines in both apex and leaf tip tissues (Fig. 6c,d). These results indicated that *ZmMADS69* may have been a target of selection in the adaptation of maize to temperate regions. Taken together, we conclude that the *ZmMADS69-ZmRap2.7-ZCN8* regulatory module was targeted by selection and may therefore have played an important role in the adaptation of maize to higher latitudes.

In conclusion, we report the identification and characterization of *ZmMADS69*, which underlies an important QTL controlling the difference in flowering time between maize and its wild ancestor, teosinte. Increased expression of *ZmMADS69* is significantly associated with earlier flowering in natural populations. We demonstrated that *ZmMADS69* is a constitutive flowering activator by downregulating the expression of *ZmRap2.7*, thereby relieving repression of *ZCN8*, resulting in earlier flowering. Finally, we provide evidence that the entire *ZmMADS69-ZmRap2.7-ZCN8* regulatory module was targeted by selection for flowering time during the expansion of maize from the tropics.

Acknowledgements

We thank John Doebley (Department of Genetics, University of Wisconsin), Xiaohong Yang (National Maize Improvement Center of China, China Agricultural University), the USDA National Plant Germplasm System and the Maize Genetics COOP Stock

Center for providing the teosinte materials and the UniformMu mutant, respectively. This research was supported by the National Natural Science Foundation of China (31771806 and 91535108), the National Key Research and Development Program of China (2016YFD0100303 and 2016YFD0100404), the Recruitment Program of Global Experts and the Fundamental Research Funds for the Central Universities.

Author contributions

YL, QL, XW, PSS and FT designed the research; YL, QL, XW, CH, SH, SL, H Y L, and CL performed molecular experiments; YL, QL, GX, H-Y L, DX, LW, CW, WW, JX and XH collected phenotypic data; JL and WS performed transgenic experiments; YL, QL, XW, PSS and FT analyzed data and wrote the manuscript; All authors read and approved the final manuscript. YL, QL and XW contributed equally to this work.

ORCID

Xu Han http://orcid.org/0000-0002-2702-2520
Stefan Hey http://orcid.org/0000-0002-0416-8893
Yameng Liang http://orcid.org/0000-0002-0104-0413
Hung-Ying Lin http://orcid.org/0000-0003-3921-3946
Qiang Liu http://orcid.org/0000-0002-9402-0226
Patrick S. Schnable http://orcid.org/0000-0001-9169-5204
Feng Tian http://orcid.org/0000-0003-3552-4536
Guanghui Xu http://orcid.org/0000-0001-7986-7077
Xufeng Wang http://orcid.org/0000-0001-9345-827X

References

Abe M, Kobayashi Y, Yamamoto S, Daimon Y, Yamaguchi A, Ikeda Y, Ichinoki H, Notaguchi M, Goto K, Araki T. 2005. FD, a bZIP protein mediating signals from the floral pathway integrator FT at the shoot apex. *Science* **309**: 1052–1056.

Alter P, Bircheneder S, Zhou LZ, Schluter U, Gahrtz M, Sonnewald U, Dresselhaus T. 2016. Flowering time-regulated genes in maize include the transcription factor *ZmMADS1*. *Plant Physiology* **172**: 389–404.

Anders S, Pyl PT, Huber W. 2015. HTSeq–a Python framework to work with high-throughput sequencing data. *Bioinformatics* **31**: 166–169.

Austin DF, Lee M. 1996. Genetic resolution and verification of quantitative trait loci for flowering and plant height with recombinant inbred lines of maize. *Genome* **39**: 957–968.

Belhaj K, Chaparro-Garcia A, Kamoun S, Patron NJ, Nekrasov V. 2015. Editing plant genomes with CRISPR/Cas9. *Current Opinion in Biotechnology* **32**: 76–84.

Benjamini Y, Hochberg Y. 1995. Controlling the false discovery rate – a practical and powerful approach to multiple testing. *Journal of the Royal Statistical Society Series B-Methodological* **57**: 289–300.

Blümel M, Dally N, Jung C. 2015. Flowering time regulation in crops-what did we learn from Arabidopsis? *Current Opinion in Biotechnology* **32**: 121–129.

Bolger AM, Lohse M, Usadel B. 2014. Trimmomatic: a flexible trimmer for Illumina sequence data. *Bioinformatics* **30**: 2114–2120.

Briggs WH, McMullen MD, Gaut BS, Doebley J. 2007. Linkage mapping of domestication loci in a large maize teosinte backcross resource. *Genetics* **177**: 1915–1928.

Buckler ES, Holland JB, Bradbury PJ, Acharya CB, Brown PJ, Browne C, Ersoz E, Flint-Garcia S, Garcia A, Glaubitz JC *et al.* 2009. The genetic architecture of maize flowering time. *Science* **325**: 714–718.

Bukowski R, Guo X, Lu Y, Zou C, He B, Rong Z, Wang B, Xu D, Yang B, Xie C *et al.* 2018. Construction of the third-generation *Zea mays* haplotype map. *Gigascience* **7**: 1–12.

Castelletti S, Tuberosa R, Pindo M, Salvi S. 2014. A MITE transposon insertion is associated with differential methylation at the maize flowering time QTL *Vgt1*. *G3: Genes, Genomes, Genetics* **4**: 805–812.

Chardon F, Virlon B, Moreau L, Falque M, Joets J, Decousset L, Murigneux A, Charcosset A. 2004. Genetic architecture of flowering time in maize as inferred from quantitative trait loci meta-analysis and synteny conservation with the rice genome. *Genetics* **168**: 2169–2185.

Colasanti J, Yuan Z, Sundaresan V. 1998. The *indeterminate* gene encodes a zinc finger protein and regulates a leaf-generated signal required for the transition to flowering in maize. *Cell* **93**: 593–603.

Coles ND, McMullen MD, Balint-Kurti PJ, Pratt RC, Holland JB. 2010. Genetic control of photoperiod sensitivity in maize revealed by joint multiple population analysis. *Genetics* **184**: 799–812.

Danilevskaya ON, Meng X, Selinger DA, Deschamps S, Hermon P, Vansant G, Gupta R, Ananiev EV, Muszynski MG. 2008. Involvement of the MADS-box gene *ZMM4* in floral induction and inflorescence development in maize. *Plant Physiology* **147**: 2054–2069.

Doebley J. 2004. The genetics of maize evolution. *Annual Review of Genetics* **38**: 37–59.

Dong Z, Danilevskaya O, Abadie T, Messina C, Coles N, Cooper M. 2012. A gene regulatory network model for floral transition of the shoot apex in maize and its dynamic modeling. *PLoS ONE* **7**: e43450.

Doudna JA, Charpentier E. 2014. Genome editing. The new frontier of genome engineering with CRISPR-Cas9. *Science* **346**: 1258096.

Ducrocq S, Giauffret C, Madur D, Combes V, Dumas F, Jouanne S, Coubriche D, Jamin P, Moreau L, Charcosset A. 2009. Fine mapping and haplotype structure analysis of a major flowering time quantitative trait locus on maize chromosome 10. *Genetics* **183**: 1555–1563.

Ducrocq S, Madur D, Veyrieras JB, Camus-Kulandaivelu L, Kloiber-Maitz M, Presterl T, Ouzunova M, Manicacci D, Charcosset A. 2008. Key impact of *Vgt1* on flowering time adaptation in maize: evidence from association mapping and ecogeographical information. *Genetics* **178**: 2433–2437.

Eyre-Walker A, Gaut RL, Hilton H, Feldman DL, Gaut BS. 1998. Investigation of the bottleneck leading to the domestication of maize. *Proceedings of the National Academy of Sciences, USA* **95**: 4441–4446.

Guo L, Wang X, Zhao M, Huang C, Li C, Li D, Yang C, York AM, Xue W, Xu G *et al.* 2018. Stepwise *cis*-regulatory changes in *ZCN8* contribute to maize flowering time adaptation. *Current Biology* **28**: 3005–3015.

Hall TA. 1999. BioEdit: a user-friendly biological sequence alignment editor and analysis program for Windows 95/98/NT. *Nucleic Acids Symposium Series* **41**: 95–98.

Hirsch CN, Foerster JM, Johnson JM, Sekhon RS, Muttoni G, Vaillancourt B, Penagaricano F, Lindquist E, Pedraza MA, Barry K *et al.* 2014. Insights into the maize pan-genome and pan-transcriptome. *Plant Cell* **26**: 121–135.

Huang C, Chen Q, Xu G, Xu D, Tian J, Tian F. 2016. Identification and fine mapping of quantitative trait loci for the number of vascular bundle in maize stem. *Journal of Integrative Plant Biology* **58**: 81–90.

Huang C, Sun H, Xu D, Chen Q, Liang Y, Wang X, Xu G, Tian J, Wang C, Li D *et al.* 2018. *ZmCCT9* enhances maize adaptation to higher latitudes. *Proceedings of the National Academy of Sciences, USA* **115**: E334–E341.

Hudson RR. 2002. Generating samples under a Wright–Fisher neutral model of genetic variation. *Bioinformatics* **18**: 337–338.

Hung HY, Shannon LM, Tian F, Bradbury PJ, Chen C, Flint-Garcia SA, McMullen MD, Ware D, Buckler ES, Doebley JF *et al.* 2012. *ZmCCT* and the genetic basis of day-length adaptation underlying the postdomestication spread of maize. *Proceedings of the National Academy of Sciences, USA* **109**: E1913–E1921.

Irish EE, Nelson TM. 1991. Identification of multiple stages in the conversion of maize meristems from vegetative to floral development. *Development* **112**: 891–898.

Ishida Y, Hiei Y, Komari T. 2007. *Agrobacterium*-mediated transformation of maize. *Nature Protocols* **2**: 1614–1621.

Jin M, Liu X, Jia W, Liu H, Li W, Peng Y, Du Y, Wang Y, Yin Y, Zhang X *et al.* 2018. *ZmCOL3*, a CCT gene represses flowering in maize by interfering with the circadian clock and activating expression of *ZmCCT*. *Journal of Integrative Plant Biology* **60**: 465–480.

Kremling KAG, Chen SY, Su MH, Lepak NK, Romay MC, Swarts KL, Lu F, Lorant A, Bradbury PJ, Buckler ES. 2018. Dysregulation of expression correlates with rare-allele burden and fitness loss in maize. *Nature* **555**: 520–523.

Kuleshov NN. 1933. World's diversity of phenotypes of maize. *Journal of the American Society of Agronomy* **25**: 688–700.

Kumar R, Subba A, Kaur C, Ariyadasa TU, Sharan A, Pareek A, Sopory SK, Singla-Pareek SL. 2018. OsCBSCBSPB4 is a two cystathionine-β-synthase domain-containing protein from rice that functions in abiotic stress tolerance. *Current Genomics* **19**: 50–59.

Kushwaha HR, Singh AK, Sopory SK, Singla-Pareek SL, Pareek A. 2009. Genome wide expression analysis of CBS domain containing proteins in *Arabidopsis thaliana* (L.) Heynh and *Oryza sativa* L. reveals their developmental and stress regulation. *BMC Genomics* **10**: 200.

Lazakis CM, Coneva V, Colasanti J. 2011. *ZCN8* encodes a potential orthologue of *Arabidopsis* FT florigen that integrates both endogenous and photoperiod flowering signals in maize. *Journal of Experimental Botany* **62**: 4833–4842.

Li D, Wang X, Zhang X, Chen Q, Xu G, Xu D, Wang C, Liang Y, Wu L, Huang C *et al.* 2016. The genetic architecture of leaf number and its genetic relationship to flowering time in maize. *New Phytologist* **210**: 256–268.

Li YX, Li C, Bradbury PJ, Liu X, Lu F, Romay CM, Glaubitz JC, Wu X, Peng B, Shi Y *et al.* 2016. Identification of genetic variants associated with maize flowering time using an extremely large multi-genetic background population. *The Plant Journal* **86**: 391–402.

Librado P, Rozas J. 2009. DnaSP v5: a software for comprehensive analysis of DNA polymorphism data. *Bioinformatics* **25**: 1451–1452.

Lin HY, Liu Q, Li X, Yang J, Liu S, Huang Y, Scanlon MJ, Nettleton D, Schnable PS. 2017. Substantial contribution of genetic variation in the expression of transcription factors to phenotypic variation revealed by eRD-GWAS. *Genome Biology* **18**: 192.

Mascheretti I, Turner K, Brivio RS, Hand A, Colasanti J, Rossi V. 2015. Florigen-encoding genes of day-neutral and photoperiod-sensitive maize are regulated by different chromatin modifications at the floral transition. *Plant Physiology* **168**: 1351–1363.

Matsuoka Y, Vigouroux Y, Goodman MM, Sanchez GJ, Buckler E, Doebley J. 2002. A single domestication for maize shown by multilocus microsatellite genotyping. *Proceedings of the National Academy of Sciences, USA* **99**: 6080–6084.

McCarty DR, Settles AM, Suzuki M, Tan BC, Latshaw S, Porch T, Robin K, Baier J, Avigne W, Lai J. 2005. Steady-state transposon mutagenesis in inbred maize. *The Plant Journal* **44**: 52–61.

Meng X, Muszynski MG, Danilevskaya ON. 2011. The *FT*-like *ZCN8* gene functions as a floral activator and is involved in photoperiod sensitivity in maize. *Plant Cell* **23**: 942–960.

Minow MAA, Avila LM, Turner K, Ponzoni E, Mascheretti I, Dussault FM, Lukens L, Rossi V, Colasanti J. 2018. Distinct gene networks modulate floral induction of autonomous maize and photoperiod-dependent teosinte. *Journal of Experimental Botany* **69**: 2937–2952.

Mou S, Shi L, Lin W, Liu Y, Shen L, Guan D, He S. 2015. Over-expression of rice CBS domain containing protein, *OsCBSX3*, Confers rice resistance to *Magnaporthe oryzae* inoculation. *International Journal of Molecular Sciences* **16**: 15903–15917.

Muszynski MG, Dam T, Li B, Shirbroun DM, Hou ZL, Bruggemann E, Archibald R, Ananiev EV, Danilevskaya ON. 2006. *Delayed flowering1* encodes a basic leucine zipper protein that mediates floral inductive signals at the shoot apex in maize. *Plant Physiology* **142**: 1523–1536.

Pertea M, Kim D, Pertea GM, Leek JT, Salzberg SL. 2016. Transcript-level expression analysis of RNA-seq experiments with HISAT, StringTie and Ballgown. *Nature Protocols* **11**: 1650–1667.

Pfeifer B, Wittelsburger U, Ramos-Onsins SE, Lercher MJ. 2014. PopGenome: an efficient Swiss army knife for population genomic analyses in R. *Molecular Biology and Evolution* **31**: 1929–1936.

Rapaport F, Khanin R, Liang Y, Pirun M, Krek A, Zumbo P, Mason CE, Socci ND, Betel D. 2013. Comprehensive evaluation of differential gene expression analysis methods for RNA-seq data. *Genome Biology* **14**: R95.

Ribaut JM, Hoisington DA, Deutsch JA, Jiang C, Gonzalez-de-Leon D. 1996. Identification of quantitative trait loci under drought conditions in tropical maize. 1. Flowering parameters and the anthesis-silking interval. *Theoretical and Applied Genetics* **92**: 905–914.

Robinson MD, McCarthy DJ, Smyth GK. 2010. edgeR: a Bioconductor package for differential expression analysis of digital gene expression data. *Bioinformatics* **26**: 139–140.

Romay MC, Millard MJ, Glaubitz JC, Peiffer JA, Swarts KL, Casstevens TM, Elshire RJ, Acharya CB, Mitchell SE, Flint-Garcia SA *et al.* 2013. Comprehensive genotyping of the USA national maize inbred seed bank. *Genome Biology* **14**: R55.

Romero Navarro JA, Willcox M, Burgueno J, Romay C, Swarts K, Trachsel S, Preciado E, Terron A, Delgado HV, Vidal V *et al.* 2017. A study of allelic diversity underlying flowering-time adaptation in maize landraces. *Nature Genetics* **49**: 476–480.

Salvi S, Corneti S, Bellotti M, Carraro N, Sanguineti MC, Castelletti S, Tuberosa R. 2011. Genetic dissection of maize phenology using an intraspecific introgression library. *BMC Plant Biology* **11**: 4.

Salvi S, Sponza G, Morgante M, Tomes D, Niu X, Fengler KA, Meeley R, Ananiev EV, Svitashev S, Bruggemann E *et al.* 2007. Conserved noncoding genomic sequences associated with a flowering-time quantitative trait locus in maize. *Proceedings of the National Academy of Sciences, USA* **104**: 11376–11381.

Salvi S, Tuberosa R, Chiapparino E, Maccaferri M, Veillet S, van Beuningen L, Isaac P, Edwards K, Phillips RL. 2002. Toward positional cloning of *Vgt1*, a QTL controlling the transition from the vegetative to the reproductive phase in maize. *Plant Molecular Biology* **48**: 601–613.

Schmittgen TD, Livak KJ. 2008. Analyzing real-time PCR data by the comparative CT method. *Nature Protocols* **3**: 1101–1108.

Schnable PS, Ware D, Fulton RS, Stein JC, Wei F, Pasternak S, Liang C, Zhang J, Fulton L, Graves TA *et al.* 2009. The B73 maize genome: complexity, diversity, and dynamics. *Science* **326**: 1112–1115.

Settles AM, Holding DR, Tan BC, Latshaw SP, Liu J, Suzuki M, Li L, O'Brien BA, Fajardo DS, Wroclawska E *et al.* 2007. Sequence-indexed mutations in maize using the UniformMu transposon-tagging population. *BMC Genomics* **8**: 116.

Shrestha R, Gomez-Ariza J, Brambilla V, Fornara F. 2014. Molecular control of seasonal flowering in rice, *Arabidopsis* and temperate cereals. *Annals of Botany* **114**: 1445–1458.

Singh AK, Kumar R, Pareek A, Sopory SK, Singla-Pareek SL. 2012. Overexpression of rice CBS domain containing protein improves salinity, oxidative, and heavy metal tolerance in transgenic tobacco. *Molecular Biotechnology* **52**: 205–216.

Smaczniak C, Immink RG, Angenent GC, Kaufmann K. 2012. Developmental and evolutionary diversity of plant MADS-domain factors: insights from recent studies. *Development* **139**: 3081–3098.

Steinhoff J, Liu W, Reif JC, Della Porta G, Ranc N, Wurschum T. 2012. Detection of QTL for flowering time in multiple families of elite maize. *Theoretical and Applied Genetics* **125**: 1539–1551.

Tenaillon MI, U'Ren J, Tenaillon O, Gaut BS. 2004. Selection versus demography: a multilocus investigation of the domestication process in maize. *Molecular Biology and Evolution* **21**: 1214–1225.

Tian F, Stevens NM, Buckler ESt. 2009. Tracking footprints of maize domestication and evidence for a massive selective sweep on chromosome 10. *Proceedings of the National Academy of Sciences, USA* **106**(Suppl 1): 9979–9986.

Wang X, Chen Q, Wu Y, Lemmon ZH, Xu G, Huang C, Liang Y, Xu D, Li D, Doebley JF *et al.* 2018. Genome-wide analysis of transcriptional variability in a large maize-teosinte population. *Molecular Plant* **11**: 443–459.

Wigge PA, Kim MC, Jaeger KE, Busch W, Schmid M, Lohmann JU, Weigel D. 2005. Integration of spatial and temporal information during floral induction in *Arabidopsis*. *Science* **309**: 1056–1059.

Wright SI, Bi IV, Schroeder SG, Yamasaki M, Doebley JF, McMullen MD, Gaut BS. 2005. The effects of artificial selection on the maize genome. *Science* **308**: 1310–1314.

Xing HL, Dong L, Wang ZP, Zhang HY, Han CY, Liu B, Wang XC, Chen QJ. 2014. A CRISPR/Cas9 toolkit for multiplex genome editing in plants. *BMC Plant Biology* **14**: 327.

Xu DY, Wang XF, Huang C, Xu GH, Liang YM, Chen QY, Wang CL, Li D, Tian JG, Wu LS *et al.* 2017. *Glossy15* plays an important role in the divergence of the vegetative transition between maize and its progenitor, teosinte. *Molecular Plant* **10**: 1579–1583.

Xu G, Wang X, Huang C, Xu D, Li D, Tian J, Chen Q, Wang C, Liang Y, Wu Y *et al.* 2017. Complex genetic architecture underlies maize tassel domestication. *New Phytologist* **214**: 852–864.

Yang Q, Li Z, Li W, Ku L, Wang C, Ye J, Li K, Yang N, Li Y, Zhong T *et al.* 2013. CACTA-like transposable element in *ZmCCT* attenuated photoperiod sensitivity and accelerated the postdomestication spread of maize. *Proceedings of the National Academy of Sciences, USA* **110**: 16969–16974.

Yoo SD, Cho YH, Sheen J. 2007. *Arabidopsis* mesophyll protoplasts: a versatile cell system for transient gene expression analysis. *Nature Protocols* **2**: 1565–1572.

Supporting Information

Additional Supporting Information may be found online in the Supporting Information section at the end of the article:

Fig. S1 Phenotypic comparisons between NIL(maize) and NIL (8759).

Fig. S2 Protein sequences of ZmMADS69 in B73, W22 and 8759.

Fig. S3 The relationship between *ZmMADS69* expression and flowering time in 265 diverse maize inbred lines.

Fig. S4 Phenotypic comparisons between *ZmMADS69* transgene-positive and transgene-negative T_2 plants under long days.

Fig. S5 Phenotypic comparisons between *ZmMADS69* transgene-positive and transgene-negative T_1 plants under short days.

Fig. S6 Phenotypic comparisons between *ZmMADS69* homozygous mutants and heterozygous siblings planted at Ames and Boone.

Fig. S7 Subcellular localization of ZmMADS69 in *Nicotiana benthamiana* leaf epidermal cells.

Fig. S8 Summary of RNA-seq reads mapping.

Fig. S9 Clustering and multidimensional scaling (MDS) analysis of experimental samples used in RNA-seq.

Fig. S10 Knockout line of *ZmRap2.7* by CRISPR/Cas9.

Fig. S11 Knockout lines of *ZCN8* by CRISPR/Cas9.

Fig. S12 Flowering time comparison between wildtype and *ZmRap2.7* knockout line.

Fig. S13 Flowering time comparison between wildtype and *ZCN8* knock out lines.

Fig. S14 Expression analyses of *ZmMADS69* and *ZmRap2.7* in mature leaves of NILs for *ZCN8*.

Fig. S15 Nucleotide diversity (π) across the region of *ZmMADS69* gene body in diverse maize and teosinte lines.

Table S1 Fine mapping in Sanya, 2015.

Table S2 Fine mapping in Sanya, 2016.

Table S3 Molecular markers used in this study.

Table S4 Maize and teosinte materials used to sequence the fragments around *ZmMADS69*.

Table S5 Differentially expressed genes between the *ZmMADS69* transgene-positive and transgene-negative plants.

Please note: Wiley Blackwell are not responsible for the content or functionality of any Supporting Information supplied by the authors. Any queries (other than missing material) should be directed to the *New Phytologist* Central Office.